

INVESTIGATION OF TRAPPED MAGNETIC FLUX IN SUPERCONDUCTING NIOBIUM SAMPLES WITH POLARIZED NEUTRON RADIOGRAPHY

O. Kugeler[†], M. Krzyzagorski, J. Köszegi, L. Riik, R. Ziesche, W. Treimer, J. Knobloch
Helmholtz Zentrum Berlin, Berlin, Germany

Abstract

The dynamics of flux expulsion during superconducting transition and the influence of external AC magnetic fields on expulsion of trapped fields in Nb samples has been investigated with radiography using polarized neutrons. Results of these experiments are presented.

INTRODUCTION

Trapped magnetic flux is a major contribution to the residual resistance of superconducting cavities. Minimizing the trapped flux can significantly reduce operation costs of superconducting CW accelerators. In order to gain a better understanding of the mechanisms, various techniques have been employed to measure it: Field probes like fluxgates [1] or AMR sensors [2] can only indirectly measure the trapped flux, by deducing it from the change in ambient field due to incomplete Meissner transition, taking into consideration the demagnetisation behaviour of the involved sample [3] or cavity [4]. Magneto-optic methods can visualize trapped flux on a surface at good resolution better than $10\mu\text{m}$ [5-7].

We present a complimentary method, polarized neutron radiography [8-11], which measures the field directly and provides spatially resolved in-depth information from the

entire volume of the investigated sample. We apply this method to the specific questions of SRF applications. The following issues were addressed with radiographies:

- Influence of cool-down speed on the amount of trapped flux.
- Influence of applied field on trapped flux
- Influence of an AC external magnetic field on the flux trapping behaviour

EXPERIMENTAL

The presented neutron radiographies were recorded with PONTO II, an instrument of the University of Applied Sciences (Beuth Hochschule für Technik) Berlin that is operated at the BER II research reactor at HZB. PONTO II uses cold, spin-polarized neutrons at adjustable wavelengths of $2.9\text{\AA} \leq \lambda \leq 4.5\text{\AA}$. As illustrated in Figure 1, these neutrons are sent through a sample in a closed cycle cryostat that can be cooled down to $T=4.0\text{ K}$. While there is negligible scattering of neutrons in the setup, their spin interacts only with the ambient magnetic field along the neutron's path from the polarizing element, through the sample, up to the analysing element and the detector.

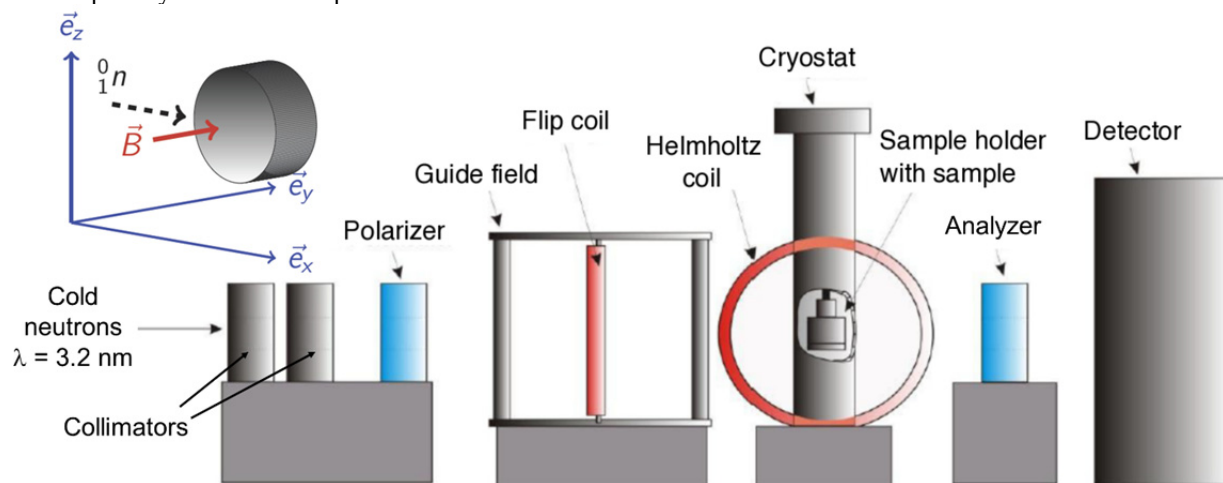


Figure 1: Setup of the PONTON II experiment: Cold neutrons from the HZB reactor BER II reactor are collimated and spin polarized. The neutrons' trajectory leads through a guide field with the option to perform a spin-flip by a flip-coil, the sample inside a cryostat, and a spin analyzer, and it ends in the detector. The spin rotates in the magnetic field of a sample and hence typically approaches the spin analyzer in a non-parallel orientation. The angle of the final spin rotation depends on the magnetic field along the neutron path. Changes in the polarization reduce the transmission through the spin analyzer which leads to contrast information of the recorded images. The influence of the guide field has to be accounted for with calibration measurements. The inset shows the orientation of sample, neutron velocity and trapped magnetic field (here: 0° position).

A flat field offset-measurement with sample in non-superconducting state allows for removing the effects of the inhomogeneous beam, attenuation of sample, sample-

holder and temperature shielding and background field. After exposure to the field, neutrons are detected in an up to $40\text{ mm} \times 40\text{ mm}$ field of view at a spatial resolution of

120 μm . The phase of the precession due to the amount of magnetic field can be detected by a second polarizer in front of the detector in multiples of 2π . A photograph of the PONTO II experiment is shown in Figure 2.

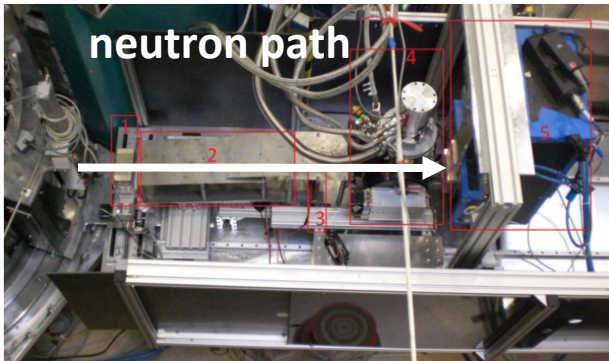


Figure 2: Photograph of the PONTO II set up from top: (1) polarizer, (2) guiding field, (3) spin flipper, (4) sample in cryostat and Helmholtz coils, and (5) neutron detector.

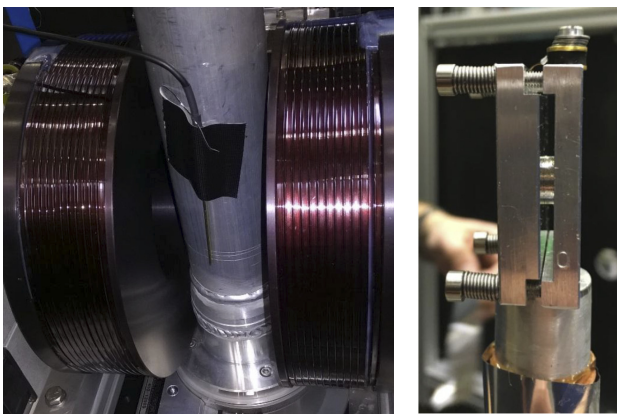


Figure 3: Left: Helmholtz coil used for field cooling of sample in cryostat. Maximum fields of 60 mT (85 mT for a short time) could be generated across the sample. Magnetic fields were measured with a Hall probe. Right: Holding frame and mounted Nb-sample.

The samples were cut from a large grain ingot of high purity RRR300 Niobium provided by Heraeus. The obtained cylindrical discs were 5 mm in radius and 5 mm in height. They received a chemical polish at DESY in a beaker. The amount of removed material by the flash (1:1:2) BCP was not monitored. Samples were mounted into an aluminum sample holder with Titanium spring-loaded bolts. The holder is shown in the right part of Figure 3. The holder was installed in the cryostat and conduction cooled via a cold trap. A Helmholtz coil around the cryostat allowed to apply a homogeneous magnetic field during phase transition, see left part of Figure 3. The field cooling was always performed by starting from a stabilized temperature above $T=15$ K above $T_c = 9.2$ K, then applying a certain cooling rate that could be varied between 0.1 K min^{-1} and 1 K min^{-1} . When a temperature of 5 K was reached the external field was turned off. The applied external field was always

oriented parallel to the cylinder's length axis. The Helmholtz coils could be operated in AC mode up to 10 Hz with arbitrary superposition of DC magnetic field offset. After the sample transitioned into the superconducting state, the coils were turned off, i.e. all samples in the experiments presented here were field-cooled.

Then the magnetic field trapped inside the superconductor was exposed to the neutron beam. In the default position (or 0° -position) the sample-axis and thus the trapped field was oriented perpendicular to the neutron beam. The sample holder could be rotated vertically by 360° . Rotating it by 90° brought the sample into a position where its axis was facing and the trapped field was oriented parallel to the neutron beam (90° position). In the tests, the cooling speed was varied between 0.1 K/min and 1 K/min as limited by the cold trap. Also, the ambient field was varied by (a) applying different DC field levels between 0 mT and 5 mT, (b) applying different AC field levels at different frequencies with (c) different superimposed DC offset levels.

For each cooling procedure a set of two radiographs in 0° and the complementary 90° position were recorded. Each radiograph required about 4 hours of exposure time.

RESULTS

The analysis and evaluation of neutron data into radiographs is described elsewhere [8]. The following results were obtained:

The cooling rate (within the limitations of the cold trap) did not influence the amount of trapped flux. The resulting images at different rates were identical, see Figure 4.

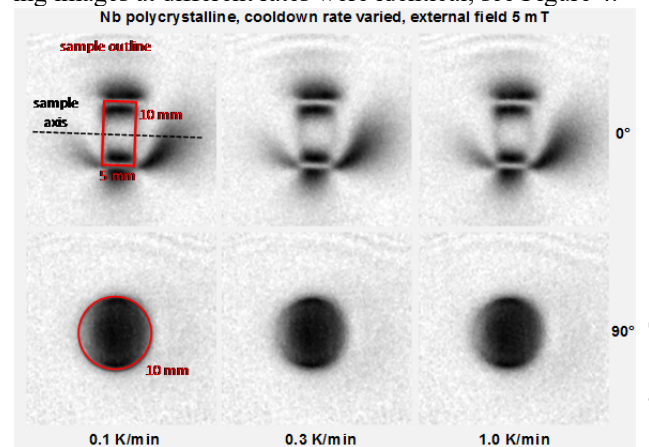


Figure 4: Cooling in external magnetic field of 5 mT at varying rates. The neutron beam is always perpendicular to the paper plane. The sample outline and dimensions are indicated in red. Upper row: 0° sample orientation, lower row: 90° sample orientation.

† email address oliver.kugeler@helmholtz-berlin.de

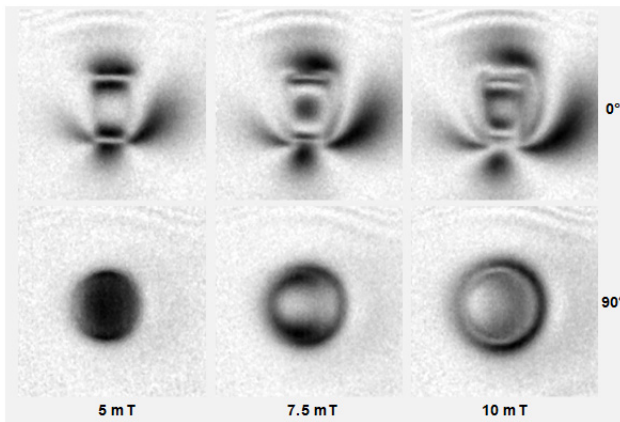


Figure 5: Cooling at various external DC-magnetic fields and cooling rate = 0.3 K/min.

The amount of trapped flux increased linearly with the amount of applied field. Figure 5 shows radiographies obtained after cooling at different ambient, static magnetic fields.

The deviation from symmetry with respect to the sample axis was due to imperfect alignment of sample, beam and detector. All measurements were performed at conditions, where the Meissner phase is the energetically lowest state, i.e. all ambient flux should have been expelled from the sample. The conceived flux lines have to perform a movement over macroscopic distances in a viscous-like medium. The viscosity is small at the critical temperature but rises quickly when lowering the temperature. These considerations have led to the

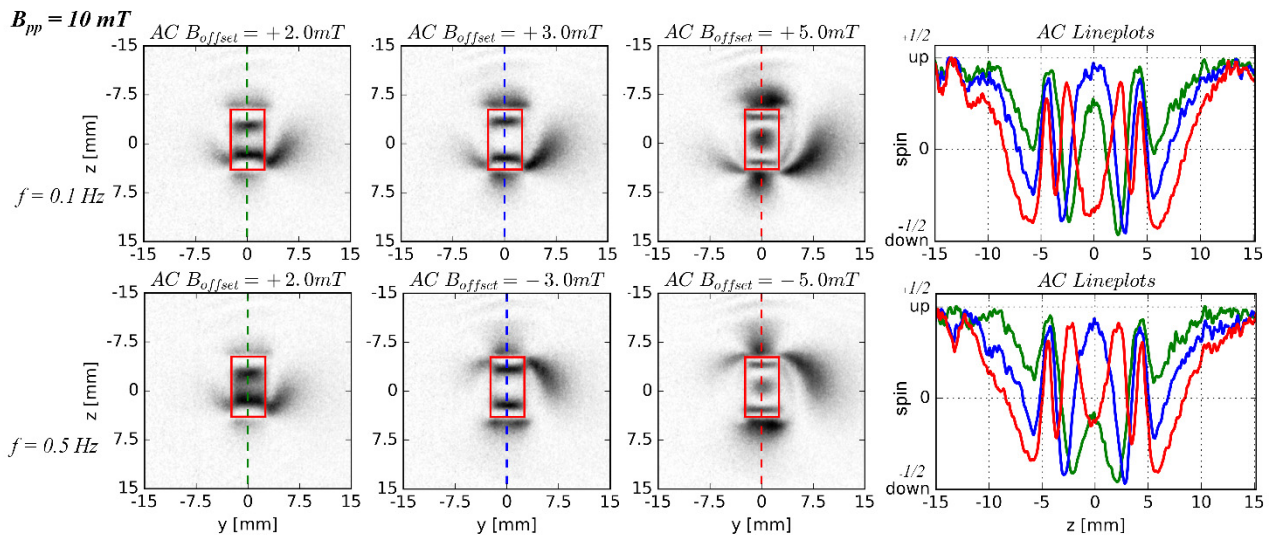


Figure 6: Radiographies of ac-field cooled sample. The field amplitude was always 10 mT peak to peak. The DC offset field and the frequency of the AC field were varied. The right graphs show the integrated spin phase change.

REFERENCES

- [1] Aull, S., O. Kugeler, and J. Knobloch, "Trapped Magnetic Flux in Superconducting Niobium Samples". *Physical Review Special Topics - Accelerators and Beams*, vol. 15, pp. 1-6, 2012.
- [2] Schmitz, B., *et al.*, "Setup of a Spatially Resolving Vector Magnetometry System for the Investigation of
- [3] Flux Trapping in Superconducting Cavities", in *Proc. IPAC 2017, Copenhagen, 2017*.
- [3] Aull, S., "Investigation of Trapped Magnetic Flux in Superconducting Niobium Samples", in *Mathematisch-Naturwissenschaftliche Fakultät I - Institut für Physik, Humboldt-Universität zu Berlin*, 2011.

experimental attempt to overlay an external alternating magnetic field over the ambient field during cool-down, that might give the flux-lines additional impetus on their path through the superconductor. The idea of that assumed mechanism is the fact that a change in sign of the magnetisation involves a zero transition where the trapping mechanism is inactive since there is no flux line present that could be trapped. The results of those efforts are shown in Figure 6: The sample was field-cooled in different external magnetic fields, 2 mT, 3 mT, and 5 mT, and an AC field with 10 mT amplitude was superimposed at 0.1 Hz, and 0.5 Hz. The measured spin-polarisation in the sample-center is plotted in the right graphs. The result of these expulsion attempts is that less flux is trapped at higher frequencies under otherwise identical conditions. The series could not be continued to even higher frequencies due to dielectric heating at the cryostat, so the results are not significant enough to make a solid statement. Also, in order to be usable as a flux removal procedure one would aim at 100% efficiency rather than the observed effect.

CONCLUSION

The flux trapping and expulsion behaviour of field-cooled samples has been investigated with neutron tomography. The amount of trapped flux was proportional to the external field and independent on cooling rate. The trapping efficiency seems to decrease with the frequency of a superimposed external AC magnetic field.

- [4] Romanenko, A., *et al.*, "Ultra-high Quality Factors in Superconducting Niobium Cavities in Ambient Magnetic Fields up to 190 mG", arXiv:1410.7877, 2014.
- [5] Vinnikov, L.Y. and A.O. Golubok, "Direct Observation of Magnetic Structure in Niobium Single Crystals with Hydride Precipitate Pinning Centres". *Phys. Stat. Sol. (a)*, vol. 69, p. 631, 1982.
- [6] Polyanskii A., *et al.*, "Magneto-Optical Investigation of Superconducting Materials", In: Johansen T.H., Shantsev D.V. (eds) *Magneto-Optical Imaging. NATO Science Series (Series II: Mathematics, Physics and Chemistry)*, vol. 142, Springer, Dordrecht, 2004.
- [7] Polyanskii, A.A., *et al.*, "Magneto-Optical Study High-Purity Niobium for Superconducting RF Application", *Symposium on the Superconducting Science and Technology of Ingot Niobium*, vol. 202, pp. 186-202, 2011.
- [8] Kardjilov, N., *et al.*, "Three-dimensional Imaging of Magnetic Fields with Polarized Neutrons". *Nature Physics*, vol. 4, pp. 399-403, 2008.
- [9] Treimer, W., O. Ebrahimi, and N. Karakas, "Observation of Partial Meissner Effect and Flux Pinning in Superconducting Lead Containing Non-superconducting Parts". *Applied Physics Letters*, vol. 101, p. 162603, 2012.
- [10] Treimer, W., O. Ebrahimi, and N. Karakas, "Imaging of Quantum Mechanical Effects in Superconductors by Means of Polarized Neutron Radiography". *Physics Procedia*, vol. 00, p. 0-10, 2011.
- [11] Treimer, W., *et al.*, "Polarized Neutron Imaging and Three-dimensional Calculation of Magnetic Flux Trapping in Bulk of Superconductors". *Physical Review B*, vol. 85, p. 184522, 2012.